Hindawi Publishing Corporation
Journal of Nanomaterials
Volume 2012, Article ID 252481, 8 pages
doi:10.1155/2012/252481

Research Article

Biphasic Osteogenic Characteristics of Human Mesenchymal Stem Cells Cultured on TiO_2 Nanotubes of Different Diameters

Kyung-Suk Moon, Sang-Hui Yu, Ji-Myung Bae, and Seunghan Oh

Department of Dental Biomaterials and Institute of Biomaterials and Implant, College of Dentistry, Wonkwang University, Iksan, Jeonbuk 570-749, Republic of Korea

Correspondence should be addressed to Seunghan Oh, shoh@wku.ac.kr

Received 1 December 2011; Accepted 10 February 2012

Academic Editor: Titipun Thongtem

We cultured human mesenchymal stem cells (hMSCs) on TiO_2 nanotubes with diameters of 30–100 nm to assess the size-effect of TiO_2 nanotubes on the behavior and osteogenic functionality of hMSCs. Most studies of the expression of genes encoding alkaline phosphatase (ALP), osteocalcin (OCN), osteopontin (OPN), and integrin-β (INT-B), after 1 week of incubation, supported the results of cell viability and MTT assays at 48 hrs of plating. However, after 2 weeks of incubation, expression of ALP, OPN, INT-B, and protein kinase R-like ER kinase (PERK) genes were significantly higher in cells cultured on 70 nm TiO_2 nanotubes than that in cells cultured on other TiO_2 nanotubes and Ti. This biphasic osteogenic characteristic of hMSCs is supposed to relating to the nature of the hMSCs adhering to the substrate at the beginning of incubation, and the nanostructural stimulation caused by the topography of TiO_2 nanotubes at a later stage of incubation. The discovery of these biphasic characteristics of hMSCs cultured on different-sized TiO_2 nanotubes may contribute to resolving the discrepant results relating to the size-effect of TiO_2 nanotubes on the adhesion, proliferation, and functionality of cells.

1. Introduction

The development of titanium dioxide (TiO_2) nanostructures has been a focus of many recent investigations, given the use of TiO_2 nanostructures in the field of photocatalysis [1–3], solar cells [4], and biomedical applications [5–7]. A number of studies have compared the unique features of TiO_2 nanotubular structures on Ti to microscaled TiO_2 structures, in the development of novel solar cells and biomaterials [8–13]. Multiple reports have also demonstrated that the shape, size, wall thickness, and crystallinity of TiO_2 nanotubes affect the adhesion, proliferation and functionality of many types of cells [14–17]. Moreover, it is now well known that TiO_2 nanotubular structure induces augmented osseointegration into animal bone *in vivo* [12, 18, 19].

However, there have been some inconsistencies in the literature regarding the optimal size of TiO_2 nanotubes for eliciting maximal adhesion, proliferation, and functionality of cells [5, 6, 15, 20–22]. Furthermore, several researchers have reported that TiO_2 nanotubular structure inhibited the behavior and functionality of vascular smooth muscle cells, compared to the effect of pure Ti, regardless of the size of the nanotubes [23]. Therefore, identifying factors besides the size of the TiO_2 nanotubes that play a critical role in determining the adhesion, proliferation, and functionality of cells is crucial for resolving the incongruity regarding the size effect of TiO_2 nanotubes on cell behavior and functionality.

We have previously shown that different sterilization methods (wet autoclave versus dry autoclave) of TiO_2 nanotubes induced different osteogenic differentiation of human mesenchymal stem cells, due to the residual air trapped in the nanotubes [24]. Similarly, Zhao et al. compared several types of sterilization methods, such as autoclaving, ultraviolet (UV) radiation, and ethanol sterilization, to assess the cytocompatibility of TiO_2 nanotubes sterilized by each method and reported that UV sterilization resulted in the best cell functionality, including adhesion and proliferation [25]. However, because many experimental factors (e.g., electrolyte solution, anodization voltage, anodization time,

temperature, and specimen shape) are involved in preparation of TiO_2 nanotube arrays on a Ti surface, there are many variables that need to be considered in such in vitro and in vivo experiments.

Surface roughness is known to be a key factor determining the morphogenic effects of implant materials on adhesion, proliferation, and functionality of various types of cells [26–30], and most researchers have focused on the effect of nanotopography and morphology on the behavior and functionality of cells [31–36]. TiO_2 nanotubes manufactured on commercial Ti are mainly anodized by electrolyte solution. Commercial Ti plate is prepared by a machining and rolling process, which can lead to the formation of micro- and macroscale roughness at the surface of Ti, which can, in turn, distort the nanostructural features in the absence of further treatment. On the other hand, electropolishing of Ti leads to reduced micro- and nanoroughness (<5 nm) and a uniform flat surface [37]. TiO_2 nanotube arrays fabricated on electropolished Ti indeed have true nanotubular structure and can more precisely indicate the effect of TiO_2 nanotubes on cell behavior and functionality.

In this study, we prepared TiO_2 nanotubes with diameters of 30, 50, 70, and 100 nm on electropolished Ti, thereby minimizing factors that may interfere with nanotubular features. We used these to assess the size effect of TiO_2 nanotubes on the behavior and osteogenic functionality of hMSCs, as measured by cell viability, MTT(3-(4,5-dimethylthiazole-2-yl)-2,5-diphenyl tetrazolium bromide) assay, real-time PCR assay, and alizarin red assay.

2. Materials and Methods

2.1. TiO_2 Nanotubes Fabrication. Commercial Ti sheet (0.2 mm thick, 99.5%, Hyundai Ti, South Korea) was electropolished by electrochemical etching technique as published previously [37]. As shown Figure 1(a), electropolished Ti showed mirror surface. Electropolished Ti sheet was cleaned by acetone and D.I. (deionized) water. The nanotubes were prepared in 0.5 w/v % hydrofluoric acid (Merck, 48 w/v %, NJ, USA) in water with acetic acid (JT Baker, 98 w/v %, NJ, USA; Volumetric Ratio = 7 : 1) at 5, 10, 15, and 20 V for 20 min. A platinum electrode (DSM, 99.99%, South Korea) served as the counterpart. The samples were then rinsed with D.I. water, dried at 60°C for 24 hrs, and heat-treated at 500°C for 2 hrs to crystallize amorphous TiO_2 nanotubes into anatase structure. The morphology of TiO_2 nanotube arrays was observed by field emission scanning electron microscope (FE-SEM; S4800, Hitachi, Japan). The crystalline phases of TiO_2 nanotube arrays were determined by X-ray diffractometer (XRD; X'Pert PRO MRD, PANalytical B.V., Netherlands) with Ni-filtered Cu-Kα ray. The glancing angle of the specimen was fixed at 5° against the incident beam enabling the detection of XRD patterns to be the depth of less than 5 μm from the top surface of the substrate.

Anatase TiO_2 nanotube specimens were cut into $1.27 * 1.27\ cm^2$ and sterilized by wet autoclaving method as previously reported [24]. And then, wet-autoclaved samples were sterilized by using ultraviolet (UV) radiation. An electropolished Ti sheet cut into identical sized pieces was used as a control and was autoclaved by the same methods.

2.2. hMSCs Cell Culture. Human mesenchymal stem cells (hMSCs) were obtained from Lonza Corporation (Poietics hMSCs, Switzerland). The cell growth media were composed of α-MEM (Invitrogen, CA, USA), 10% Fetal Bovine Serum (FBS) (Invitrogen), 1% penicillin-streptomycin (Invitrogen). The cell suspension was plated in a cell culture dish and incubated under 37°C, 5% CO_2 environment. All experiments of hMSCs were conducted with cultures at passage 4-5. When hMSCs showed high confluence, they were seeded onto TiO_2 nanotube experimental substrate placed on a 12-well plate with the density of 25,000 cells/well and stored in a CO_2 incubator for each incubation time. Also, osteogenic induction media (cell growth media including 10 mM β-glycerol phosphate (Sigma Co., MO, USA), 150 μg/mL ascorbic acid (Sigma), and 10 nM dexamethasone (Sigma) were added to promote the osteogenic differentiation of hMSCs after 3 days of incubation. Osteogenic induction media were changed every 2-3 days.

2.3. Cell Viability Test. Fluorescein diacetate (FDA; Sigma, MO, USA) staining technique was performed to count viable hMSCs adhered to the specimen. At 2, 24, and 48 hrs after plating, hMSCs on the substrates were rinsed with phosphate-buffered saline solution (PBS) (Invitrogen, CA, USA) and incubated with FDA working solution (50 μg FDA dissolved in 10 mL PBS solution) for 30 seconds and then washed three times by PBS solution. The washed specimens were pictured by an inverted fluorescence microscope (CKX41, Olympus Co., Japan). We tested 2 samples per experimental group for cell adhesion and proliferation test and counted the number of cells adhered at 4 corners of a specimen and a center of a specimen.

2.4. MTT Assay. After the selected incubation periods, the samples were washed by PBS solution and transferred to a new 12-well plate. 1 mL of MTT dye agent (Sigma) was added to each well. After 3 hours of incubation in 5% CO_2 incubator, 1 mL of isopropanol was added to each well and 12-well plate was shaken for 30 minutes. The absorbance of each solution was measured at the wavelength of 570 nm by microplate ELISA reader (Spectra Max 250, Thermo Electron Co., USA).

2.5. Real-Time PCR Assay. After 1 and 2 weeks of culture, total RNA of the cells cultured on the experimental substrates were extracted by TRI agent (Invitrogen) and reverse-transcribed into cDNA by cDNA Synthesis Kit (SuperScript VILO; Invitrogen). Real-time PCR was performed by SYBR Green Dye-Based Gene Expression Assays (Invitrogen), and the information of PCR primer used in this study is listed in Table 1. Real-time PCR was carried out by using StepOne Real-Time PCR System (Applied Biosystems, USA). cDNA samples (1 μL for total volume of 20 μL) were analyzed

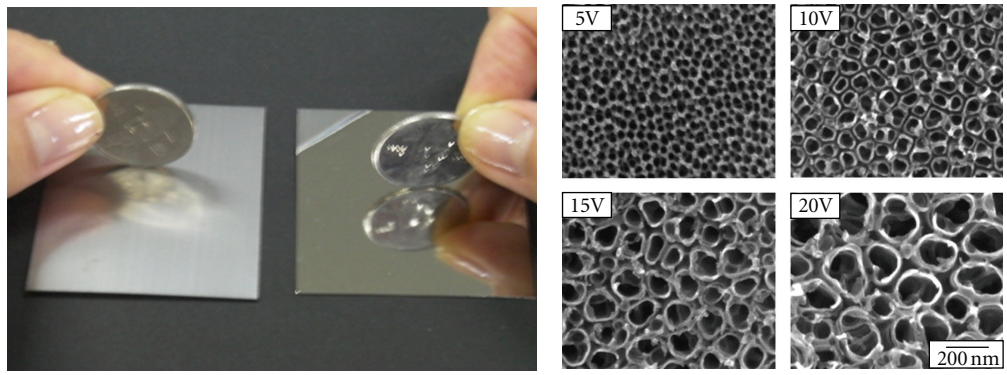

(a) (b)

Figure 1: (a) The photograph of commercial Ti (a) and electropolished Ti (b), (b) SEM micrographs of heat-treated TiO_2 nanotubes with different diameters. The images show highly ordered nanotubes with four different pore sizes between 30 and 100 nm.

Table 1: Primer sequences used in real-time PCR.

Target	Sequences
GAPDH	Forward 5′-CAA TGA CCC CTT CAT TGA CC-3′
	Reverse 5′-GAC AAG CTT CCC GTT CTC AG-3′
Osteopontin	Forward 5′-AAG CGA GGA GTT GAA TGG-3′
	Reverse 5′-GGA AAG TTC CTG ACT ATC-3′
Alkaline phosphatase	Forward 5′-ATC TTT GGT CTG GCC CCC ATG-3′
	Reverse 5′-ATG CAG GCT GCA TAC GCC AT-3′
Osteocalcin	Forward 5′-CGC AGC CAC CGA GAC ACC AT-3′
	Reverse 5′-AGG GCA AGG GGA AGA GGA AAG AA-3′
PERIK	Forward 5′ CCG AAG CCA CCT TGT CTA CC-3′
	Reverse 5′-TTC ATC CTG GTC CAT TGC AG-3′
ATF 6	Forward 5′-TCA GCT GAT GGC TGT CCA GT-3′
	Reverse 5′-TGA TGT GGA GGA TCC TGG TG-3′

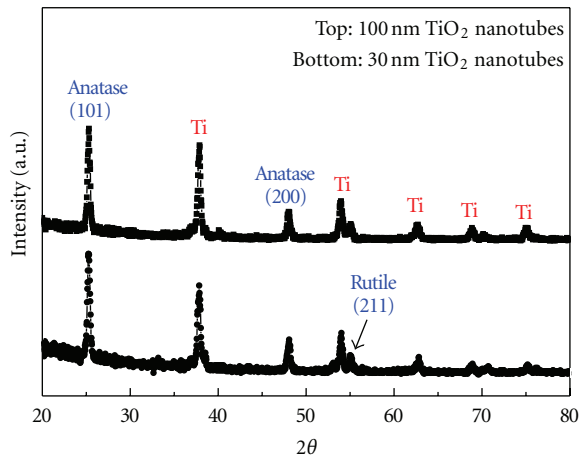

Figure 2: X-ray diffraction patterns of heat-treated 30 nm and 100 nm TiO_2 nanotubes.

for gene of interest and for house-keeping gene GAPDH. Cycle-threshold point was compared to quantify the gene expression level of each sample. All levels of expression of experimental group were normalized by the level of expression of control group (hMSCs cultured on pure Ti).

2.6. Alizarin Red Assay. After 3 weeks of incubation, the samples were rinsed with PBS solution and fixed with 4% paraformaldehyde solution (Sigma) at room temperature for 20 min. After fixation, the samples were stained with alizarin red solution (Sigma) for 20 min and then washed twice with D.I. water. The stained sample was photographed by inverted microscope (CKX 41, Olympus, Japan) to observe the formation of bone nodule. Then, the sample was reacted with 10% acetic acid (JT Baker, USA) for 30 min and stored at 85°C for 10 min. After heating, solution was collected from the sample and centrifuged at 11,000 rpm for 15 min. Supernatant was collected from the solution after centrifugation. Same volume of 10% ammonium hydroxide (Sigma) was added to the solution in order to neutralize the supernatant. The absorbance of each solution was measured at the wavelength of 405 nm by microplate ELISA reader (Spectra Max 250, Thermo Electron Co., USA).

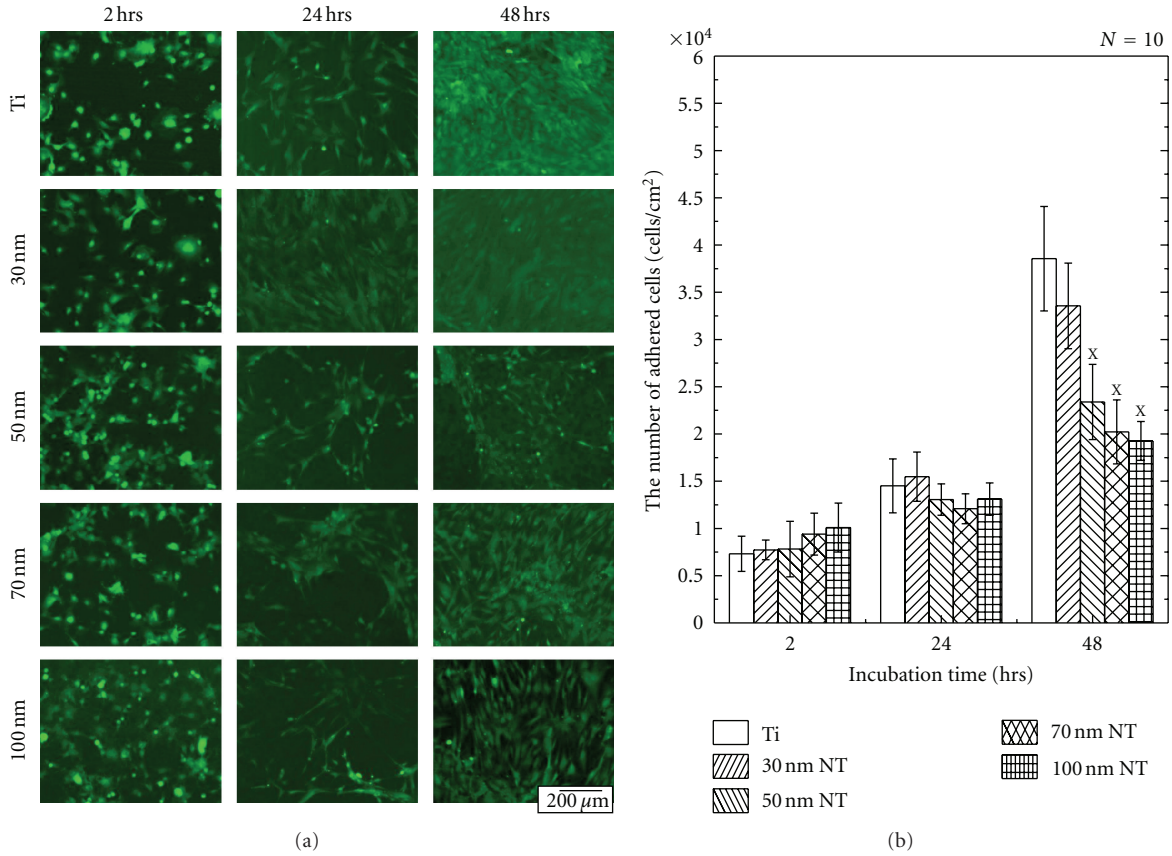

Figure 3: (a) Fluorescein diacetate (FDA) images of live osteoblast cultured on Ti and 30, 50, 70, 100 nm TiO_2 nanotube. (b) The number of adhered osteoblast to Ti and 30, 50, 70, 100nm TiO_2 nanotube as a function of incubation time. #Cell seeding density = 25,000 cells/well in 12 culture wells.

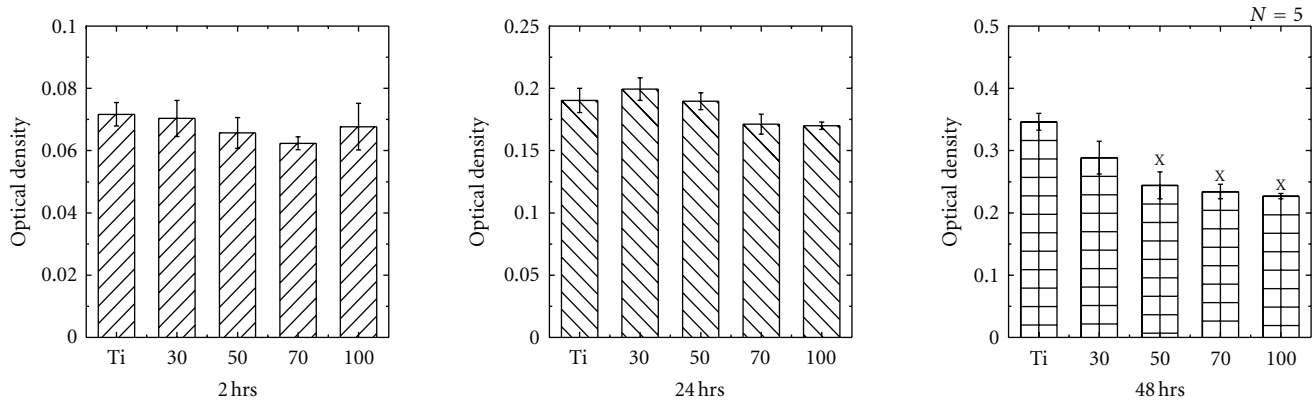

Figure 4: MTT assay for cell viability and proliferation showing the optical density of the reaction product of the MTT working solution with human mesenchymal stem cells cultured on nanotubular surface as a function of incubation time. x The data of control group (Ti) was significantly higher than that of experimental (TiO_2 nanotubes) group ($P < 0.05$).

2.7. Data Analysis. In terms of cell adhesion, MTT, and alizarin red assay, all data were expressed as mean ± standard deviation and analyzed statistically by one-way ANOVA (SPSS 12.0, SPSS GmbH, Germany) and Duncan's multiple range test as a post hoc test. Significant difference was determined at P values at least less than 0.05.

3. Results and Discussion

Figure 1(a) shows the difference in appearance between commercial Ti and electropolished Ti surfaces, whereas Figure 1(b) indicates the scanning electron microscopy (SEM) images of heat-treated 30, 50, 70, and 100 nm TiO_2 nanotubes, respectively. The micrographs show highly

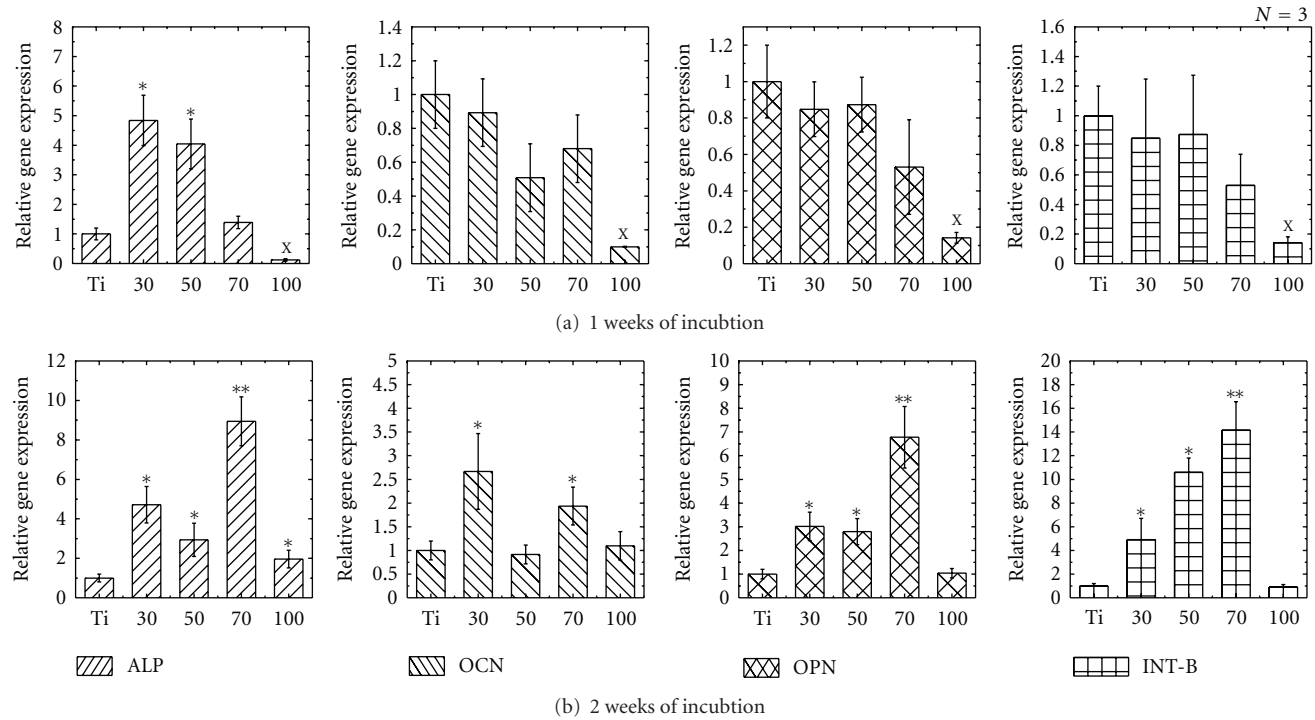

Figure 5: Quantitative PCR analysis for alkaline phosphatase (ALP), osteocalcin (OCN), osteopontin (OPN), and integrin-beta (INT-B) after 1 week and 2 weeks of incubation time. The graph shows the average ± standard deviation bars. *The data of experimental group was significantly higher than that of control group ($P < 0.05$). XThe data of control group was significantly higher than that of experimental group ($P < 0.05$). **The data was significantly the highest among all groups ($P < 0.05$).

ordered nanotubes with 4 different pore sizes, between 30 and 100 nm, created by controlling the anodization voltage across a range from 5 to 20 V, as previously reported [15].

Figure 2 indicates X-ray diffraction (XRD) patterns of heat-treated 30 and 100 nm TiO_2 nanotubes. As shown XRD results, anatase TiO_2 and Ti crystalline phases were mainly detected. Also, there was no dramatic difference of crystallinity between 30 and 100 nm TiO_2 nanotubes after heat treatment. Therefore, we did not consider the effect of nanotube crystallinity on the cell behavior and osteogenic functionality of hMSCs in this research.

Figure 3 represents images of live hMSCs stained with FDA solution and shows the number of cells adhered to the substrate. As shown in Figure 3(a), hMSCs had not yet fully spread after 2 hrs of incubation but took on an elongated appearance after 24 hrs of incubation. In Figure 3(b), it can be seen that the cell number increased over time in both the experimental and control groups; there was no significant difference between any of the TiO_2 nanotube groups after 2 hrs or after 24 hrs of incubation ($P > 0.05$).

However, by 48 hrs after plating, the number of cells adhering to 30 nm TiO_2 nanotubes was significantly higher than that adhering to 50, 70, and 100 nm TiO_2 nanotubes ($P < 0.05$; Figure 3(b)); this data showed trends similar to those of previously published data. However, in previous studies, the number of cells adhering to pure Ti within 48 hrs of incubation was significantly lower than that adhering to any of the TiO_2 nanotubes [15, 19]. In contrast, in this study, we found that the number of adherent cells cultured on electropolished Ti was significantly higher than that of cells cultured on 50, 70, and 100 nm TiO_2 nanotubes (Figure 3(b)).

Figure 4 shows the results of the MTT assay for assessing the proliferative ability of hMSCs. The data indicated a similar trend to that of the FDA-staining test. Therefore, the results of both the cell viability test and the MTT assay indicated clearly that electropolishing of Ti promotes the adhesion and proliferation of hMSCs.

In order to assess the osteogenic functionality of the cells, we performed real-time PCR analysis for alkaline phosphatase (ALP), osteocalcin (OCN), osteopontin (OPN), and integrin-β1 (INT-B) expression after 1 and 2 weeks of incubation (Figure 5). After 1 week of incubation, expression of OCN, OPN, and INT-B genes was not significantly different between the TiO_2 nanotubes of 30, 50, and 70 nm diameter and electropolished Ti; however, the expression of these genes was significantly different between these and the 100 nm TiO_2 nanotubes. Thus, the 1-week incubation real-time PCR results were mostly similar to the results of the cell viability test and the MTT assay. However, ALP gene expression in cells cultured on 30 and 50 nm TiO_2 nanotubes was significantly higher than that for cells cultured on pure Ti ($P < 0.05$; Figure 5).

Two weeks after plating, ALP, OPN, and INT-B gene expression was highest in cells cultured on 70 nm TiO_2 nanotubes ($P < 0.05$). In additions, OCN gene expression

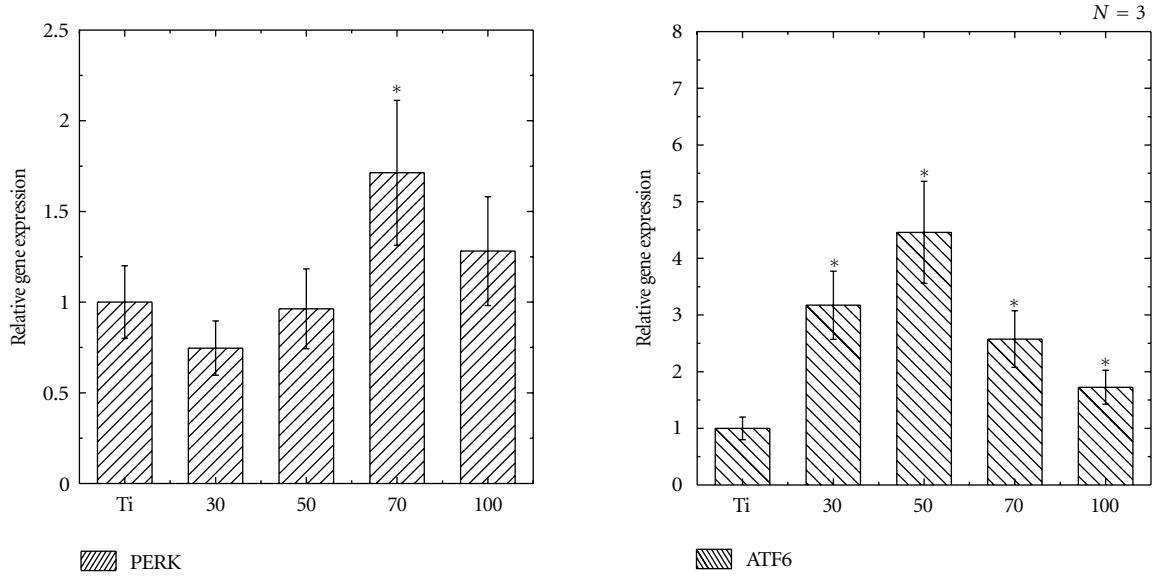

Figure 6: Quantitative PCR analysis for protein kinase R-like ER kinase (PERK) and activating transcription factor 6 (ATF6) after 2 weeks of incubation time. The graph shows the average ± standard deviation bars. *The data of experimental group was significantly higher than that of control group ($P < 0.05$).

was significantly higher in cells grown on 30 and 70 nm TiO_2 nanotubes than in cells cultured on other TiO_2 nanotubes and Ti (Figure 5).

Typically, after incubation commences, osteogenic characteristics should be manifested only by hMSCs adhering to the substrate. However, the results of real-time PCR analysis indicated that, after the early stages of incubation, hMSCs reacted to the nanostructural stimulation of the TiO_2 nanotubes and altered their osteogenic functionality according to the size of TiO_2 nanotubes.

We also investigated expression of protein kinase R-like ER kinase (PERK) and activating transcription factor 6 (ATF6), which are known to promote osteoblast differentiation of hMSCs, by real-time PCR (Figure 6). PERK gene expression was slightly, although significantly, higher in cells cultured on 70 nm TiO_2 nanotubes than in those grown on other TiO_2 nanotubes or Ti. Additionally, the expression of ATF6 was significantly higher in cells grown on any of the TiO_2 nanotubes than in cells grown on Ti (Figure 6).

Many studies have reported that bone morphogenetic protein 2 (BMP2) activates unfolded protein response (UPR) transducers, such as PERK, ATF6, and OASIS, as BMP2 treatment dramatically promotes the expression of ATF6, with a concomitant increase in ALP and OCN expression [38–41]. Even though we did not use BMP2 to enhance osteogenic differentiation of hMSCs in this study, the results of PERK and ATF6 gene expression lead us to speculate that PERK and ATF6 regulate ALP, OCN, and OPN transcription. In future studies, we intend to resolve the relationship between the promotion of osteogenic differentiation in hMSCs by UPR transducers and physical-mechanical stimuli, such as those arising from the nanotopography of TiO_2 nanotubes.

The result of the alizarin red assay, as shown in Figure 7, indicated that the calcific deposition in cells grown on 50, 70, and 100 nm TiO_2 nanotubes was significantly higher than that in cells grown on 30 nm TiO_2 nanotubes and Ti. These results supported those of the real-time PCR assays showing that cells grown on 70 nm TiO_2 nanotube have higher ALP, OCN, PERK, and ATF6 gene expression than cells grown on other TiO_2 nanotubes. In terms of showing high value of 100 nm TiO_2 nanotubes after 3 weeks of incubation, we are undergoing to resolve this phenomenon.

Therefore, we can surmise that the biphasic osteogenic characteristics of hMSCs might arise from the interplay of the osteogenic functionality of hMSCs that adhere to the substrate in the early stage of incubation, as well as that caused by nanostructural stimulation that varies according to the size of TiO_2 nanotubes. In order to more thoroughly investigate the effects of geometrical or topographical parameters of TiO_2 nanotubes on cell behavior as a function of incubation time, external factors, such as cell-ECM interaction, cell-cell communication, and physicochemical and mechanical stimuli, should be carefully considered.

4. Summary

The biphasic osteogenic characteristics of hMSCs cultured on different sizes of TiO_2 nanotubes have been investigated here. We found that, after 48 hrs of incubation, hMSCs cultured on Ti and 30 nm diameter TiO_2 nanotubes showed higher adhesion and proliferation than those cultured on 50, 70, and 100 nm diameter TiO_2 nanotubes. Most of the gene expression studies performed after 1 week of incubation supported results from cell viability and MTT assays at 48 hrs of plating. However, after 2 weeks of incubation, ALP, OPM, INT-B, and PERK gene expression was higher in cells cultured on 70 nm TiO_2 nanotubes than in cells cultured on other TiO_2 nanotubes or Ti. We propose that

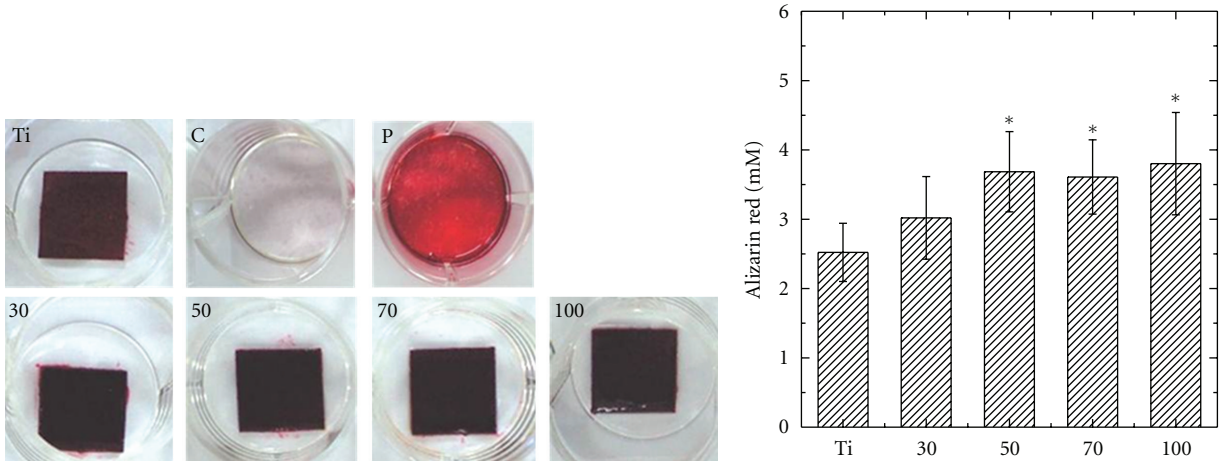

Figure 7: Alizarin red assay of hMSCs cultured on flat Ti and various sized TiO_2 nanotubes after 3 weeks of incubation. *The data of experimental group was significantly higher than that of control group ($P < 0.05$).

this was due to the interplay of osteogenic characteristics of hMSCs adhered to the substrate at the beginning of incubation and those caused by nanostructural stimulation in response to the stimulation provided by the different-sized TiO_2 nanotubes at a later stage of incubation. We conclude that these biphasic features of hMSCs cultured on different sizes of TiO_2 nanotubes may help resolve conflicts relating to the effect of the size of TiO_2 nanotubes on the adhesion, proliferation, and functionality of cells.

Acknowledgments

This research was supported by Basic Science Research Program through the National Research Foundation of Korea (NRF) funded by the Ministry of Education, Science and Technology (2010–0015443). The authors also thank the Wonkwang University of Regional Innovation Center For Next Generation Industrial Radiation Technology for the use of FE-SEM and XRD.

References

[1] S. Liu and A. Chen, "Coadsorption of horseradish peroxidase with thionine on TiO_2 nanotubes for biosensing," *Langmuir*, vol. 21, no. 18, pp. 8409–8413, 2005.

[2] M. Paulose, K. Shankar, S. Yoriya et al., "Anodic growth of highly ordered TiO_2 nanotube arrays to 134 μm in length," *Journal of Physical Chemistry B*, vol. 110, no. 33, pp. 16179–16184, 2006.

[3] H. Zhang, P. Liu, X. Liu et al., "Fabrication of highly ordered TiO_2 nanorod/nanotube adjacent arrays for photoelectrochemical applications," *Langmuir*, vol. 26, no. 13, pp. 11226–11232, 2010.

[4] K. Shankar, G. K. Mor, H. E. Prakasam, O. K. Varghese, and C. A. Grimes, "Self-assembled hybrid polymer-TiO_2 nanotube array heterojunction solar cells," *Langmuir*, vol. 23, no. 24, pp. 12445–12449, 2007.

[5] M. Bigerelle, K. Anselme, B. Noël, I. Ruderman, P. Hardouin, and A. Iost, "Improvement in the morphology of Ti-based surfaces: a new process to increase in vitro human osteoblast response," *Biomaterials*, vol. 23, no. 7, pp. 1563–1577, 2002.

[6] B. D. Boyan, T. W. Hummert, D. D. Dean, and Z. Schwartz, "Role of material surfaces in regulating bone and cartilage cell response," *Biomaterials*, vol. 17, no. 2, pp. 137–146, 1996.

[7] C. G. Galbraith and M. P. Sheetz, "Forces on adhesive contacts affect cell function," *Current Opinion in Cell Biology*, vol. 10, no. 5, pp. 566–571, 1998.

[8] C. S. Rustomji, C. J. Frandsen, S. Jin, and M. J. Tauber, "Dye-sensitized solar cell constructed with titanium mesh and 3-D array of TiO_2 nanotubes," *Journal of Physical Chemistry B*, vol. 114, no. 45, pp. 14537–14543, 2010.

[9] N. Wang, H. Li, W. Lü et al., "Effects of TiO_2 nanotubes with different diameters on gene expression and osseointegration of implants in minipigs," *Biomaterials*, vol. 32, no. 29, pp. 6900–6911, 2011.

[10] Y. T. Sul, "Electrochemical growth behavior, surface properties, and enhanced in vivo bone response of TiO_2 nanotubes on microstructured surfaces of blasted, screw-shaped titanium implants," *International Journal of Nanomedicine*, vol. 5, no. 1, pp. 87–100, 2010.

[11] L. Peng, A. D. Mendelsohn, T. J. LaTempa, S. Yoriya, C. A. Grimes, and T. A. Desai, "Long-Term small molecule and protein elution from TiO_2 nanotubes," *Nano Letters*, vol. 9, no. 5, pp. 1932–1936, 2009.

[12] C. Von Wilmowsky, S. Bauer, R. Lutz et al., "In vivo evaluation of anodic TiO_2 nanotubes; an experimental study in the pig," *Journal of Biomedical Materials Research B*, vol. 89, no. 1, pp. 165–171, 2009.

[13] G. Balasundaram, C. Yao, and T. J. Webster, "TiO_2 nanotubes functionalized with regions of bone morphogenetic protein-2 increases osteoblast adhesion," *Journal of Biomedical Materials Research A*, vol. 84, no. 2, pp. 447–453, 2008.

[14] K. S. Brammer, S. Oh, C. J. Cobb, L. M. Bjursten, H. V. D. Heyde, and S. Jin, "Improved bone-forming functionality on diameter-controlled TiO_2 nanotube surface," *Acta Biomaterialia*, vol. 5, no. 8, pp. 3215–3223, 2009.

[15] S. Oh, K. S. Brammer, Y. S. J. Li et al., "Stem cell fate dictated solely by altered nanotube dimension," *Proceedings of the National Academy of Sciences of the United States of America*, vol. 106, no. 7, pp. 2130–2135, 2009.

[16] K. S. Brammer, S. Oh, J. O. Gallagher, and S. Jin, "Enhanced cellular mobility guided by TiO_2 nanotube surfaces," *Nano Letters*, vol. 8, no. 3, pp. 786–793, 2008.

[17] J. Park, S. Bauer, P. Schmuki, and K. Von Der Mark, "Narrow window in nanoscale dependent activation of endothelial cell growth and differentiation on TiO_2 nanotube surfaces," *Nano Letters*, vol. 9, no. 9, pp. 3157–3164, 2009.

[18] L. M. Bjursten, L. Rasmusson, S. Oh, G. C. Smith, K. S. Brammer, and S. Jin, "Titanium dioxide nanotubes enhance bone bonding in vivo," *Journal of Biomedical Materials Research A*, vol. 92, no. 3, pp. 1218–1224, 2010.

[19] F. Zhang, Z. Zheng, Y. Chen, X. Liu, A. Chen, and Z. Jiang, "In vivo investigation of blood compatibility of titanium oxide films," *Journal of Biomedical Materials Research*, vol. 42, no. 1, pp. 128–133, 1998.

[20] J. Park, S. Bauer, K. Von Der Mark, and P. Schmuki, "Nanosize and vitality: TiO_2 nanotube diameter directs cell fate," *Nano Letters*, vol. 7, no. 6, pp. 1686–1691, 2007.

[21] B. Smith, S. Yoriya, L. Grissom, C. Grimes, and K. Popat, "Hemocompatibility of titania nanotube arrays," *Journal of Biomedical Materials Research Part A*, vol. 95A, no. 2, pp. 350–360, 2010.

[22] J. Park, S. Bauer, K. A. Schlegel, F. W. Neukam, K. D. Von Mark, and P. Schmuki, "TiO_2 nanotube surfaces: 15 nm—an optimal length scale of surface topography for cell adhesion and differentiation," *Small*, vol. 5, no. 6, pp. 666–671, 2009.

[23] L. Peng, A. J. Barczak, R. A. Barbeau et al., "Whole genome expression analysis reveals differential effects of TiO_2 nanotubes on vascular cells," *Nano Letters*, vol. 10, no. 1, pp. 143–148, 2010.

[24] S. Oh, K. S. Brammer, K.-S. Moon, J.-M. Bae, and S. Jin, "Influence of sterilization methods on cell behavior and functionality of osteoblasts cultured on TiO_2 nanotubes," *Materials Science and Engineering C*, vol. 31, no. 5, pp. 873–879, 2011.

[25] L. Zhao, S. Mei, W. Wang, P. K. Chu, Z. Wu, and Y. Zhang, "The role of sterilization in the cytocompatibility of titania nanotubes," *Biomaterials*, vol. 31, no. 8, pp. 2055–2063, 2010.

[26] D. Yamashita, M. Machigashira, M. Miyamoto et al., "Effect of surface roughness on initial responses of osteoblast-like cells on two types of zirconia," *Dental Materials Journal*, vol. 28, no. 4, pp. 461–470, 2009.

[27] M. Ball, D. M. Grant, W. J. Lo, and C. A. Scotchford, "The effect of different surface morphology and roughness on osteoblast-like cells," *Journal of Biomedical Materials Research A*, vol. 86, no. 3, pp. 637–647, 2008.

[28] V. Borsari, G. Giavaresi, M. Fini et al., "Physical characterization of different-roughness titanium surfaces, with and without hydroxyapatite coating, and their effect on human osteoblast-like cells," *Journal of Biomedical Materials Research B*, vol. 75, no. 2, pp. 359–368, 2005.

[29] H. J. Kim, S. H. Kim, M. S. Kim et al., "Varying Ti-6A1-4V surface roughness induces different early morphologic and molecular responses in MG63 osteoblast-like cells," *Journal of Biomedical Materials Research A*, vol. 74, no. 3, pp. 366–373, 2005.

[30] X. Hu, S.-H. Park, E. S. Gil, X.-X. Xia, A. S. Weiss, and D. L. Kaplan, "The influence of elasticity and surface roughness on myogenic and osteogenic-differentiation of cells on silk-elastin biomaterials," *Biomaterials*, vol. 32, no. 34, pp. 8979–8989, 2011.

[31] G. Kaur, C. Wang, J. Sun, and Q. Wang, "The synergistic effects of multivalent ligand display and nanotopography on osteogenic differentiation of rat bone marrow stem cells," *Biomaterials*, vol. 31, no. 22, pp. 5813–5824, 2010.

[32] E. K. F. Yim, E. M. Darling, K. Kulangara, F. Guilak, and K. W. Leong, "Nanotopography-induced changes in focal adhesions, cytoskeletal organization, and mechanical properties of human mesenchymal stem cells," *Biomaterials*, vol. 31, no. 6, pp. 1299–1306, 2010.

[33] K. T. Nguyen, K. P. Shukla, M. Moctezuma, and T. Liping, "Cellular and molecular responses of smooth muscle cells to surface nanotopography," *Journal of Nanoscience and Nanotechnology*, vol. 7, no. 8, pp. 2823–2832, 2007.

[34] J. O. Gallagher, K. F. McGhee, C. D. W. Wilkinson, and M. O. Riehle, "Interaction of animal cells with ordered nanotopography," *IEEE Transactions on Nanobioscience*, vol. 1, no. 1, pp. 24–28, 2002.

[35] M. J. Dalby, M. O. Riehle, H. Johnstone, S. Affrossman, and A. S. G. Curtis, "In vitro reaction of endothelial cells to polymer demixed nanotopography," *Biomaterials*, vol. 23, no. 14, pp. 2945–2954, 2002.

[36] A. S. G. Curtis, B. Casey, J. O. Gallagher, D. Pasqui, M. A. Wood, and C. D. W. Wilkinson, "Substratum nanotopography and the adhesion of biological cells. Are symmetry or regularity of nanotopography important?" *Biophysical Chemistry*, vol. 94, no. 3, pp. 275–283, 2001.

[37] S. Yeonmi and L. Seonghoon, "Self-organized regular arrays of anodic TiO_2 nanotubes," *Nano Letters*, vol. 8, no. 10, pp. 3171–3173, 2008.

[38] A. Saito, K. Ochiai, S. Kondo et al., "Endoplasmic reticulum stress response mediated by the PERK-eIF2α-ATF4 pathway is involved in osteoblast differentiation induced by BMP2," *Journal of Biological Chemistry*, vol. 286, no. 6, pp. 4809–4818, 2011.

[39] W.-G. Jang, E.-J. Kim, D.-K. Kim et al., "BMP2 protein regulates osteocalcin expression via Runx2-mediated Atf6 gene transcription," *Journal of Biological Chemistry*, vol. 287, no. 2, pp. 905–915, 2012.

[40] S. Kousteni, "Osterix finds its master," *EMBO Reports*, vol. 12, no. 5, pp. 382–383, 2011.

[41] T. Murakami, A. Saito, S. I. Hino et al., "Signalling mediated by the endoplasmic reticulum stress transducer OASIS is involved in bone formation," *Nature Cell Biology*, vol. 11, no. 10, pp. 1205–1211, 2009.